Control of a Flexible Robot Arm: Experimental and Theoretical Results

N. G. Chalhoub
Assistant Professor,
Department of Mechanical Engineering,
University of Nevada-Reno,
Reno, Nevada 89557-0030
Assoc. Mem. ASME

A. G. Ulsoy
Associate Professor,
Department of Mechanical Engineering
and Applied Mechanics,
University of Michigan,
Ann Arbor, Mich. 48109-2125
Mem. ASME

The operation of high precision robots is severely limited by their manipulator dynamic deflection, which persists for a period of time after a move is completed. These unwanted vibrations deteriorate the end effector positional accuracy and reduce significantly the robot arm production rate. A "rigid and flexible motion controller" is derived to introduce additional damping into the flexible motion. This is done by using additional sensors to measure the compliant link vibrations and feed them back to the controller. The existing actuators at the robot joints are used (i.e., no additional actuators are introduced). The performance of the controller is tested on a dynamic model, developed in previous work, for a spherical coordinate robot arm whose last link only is considered to be flexible. The simulation results show a significant reduction in the vibratory motion. The important issue of control and observation spillover is examined and found to present no significant practical problems. Partial evaluation of this approach is performed experimentally by testing two controllers, a "rigid body controller" and a "rigid and flexible motion controller," on a single joint of a spherical coordinate, laboratory robot arm. The experimental results show a significant reduction in the end effector dynamic deflection; thus partially validating the results of the digital simulation studies.

1 Introduction

The operation of high precision robots is severely limited by their manipulator dynamic deflection, which persists for a period of time after a move is completed. The settling time required for this residual vibration delays subsequent operations, thus conflicting with the demand for increased productivity. These conflicting requirements between high speed and high accuracy have rendered the robotic assembly task a challenging research problem.

The automation of assembly tasks will be greatly enhanced if robots can operate at higher speeds with greater positioning accuracy. These goals cannot be achieved with the existing massive robot designs, which make them slow and heavy. Many robot arms are made to be massive for increased rigidity. For higher operating speeds, mechanisms should be made lightweight to reduce the driving torque requirements and to enable the robot arm to respond faster. Lightweight robot structures are also desirable for space applications. However, lighter members are more likely to elastically deform, thus making it a necessity to take into consideration the dynamic effects of the distributed link flexibility. This is because high speed operation leads to high inertial forces which in turn cause vibration and deteriorate accuracy.

To obtain an accurate dynamic model for a very flexible structure, all the coupling terms between the flexible and the rigid body motions need to be retained. This is done by using coupled reference position and elastic deformation models. The resulting equations, which represent the combined rigid and flexible motions, are coupled and very complex. They reveal the nonlinear and nonstationary characteristics inherent in robotic manipulators.

The implementation of conventional linear control techniques have led to poor performance because of both the inherent geometric nonlinearities of these systems, and the dependence of the system dynamics on the characteristic of the manipulated objects. Therefore, a sophisticated controller design is needed to ensure the desired performance of the robot.

In the control of rigid robots, adaptive, nonlinear, and optimal control techniques have been investigated. Adaptive control theory (Dubowsky and Desforges, 1979, Horowitz and Tomizuka, 1980, Landau, 1979, Balestrino et al., 1983, Lee and Lee, 1984, Donalson and Leondes, 1963) has been proposed as a promising solution to the nonlinearity and nonstationarity problems. The main task is to adjust the feedback gains of the arm controller so that its closed loop performance characteristics closely match the desired ones. However, the large required computation time has restricted the application of adaptive control strategies to simulation studies.

Nonlinear control, or the "computed torque" method (Gilbert and Ha, 1984), has led to better performance over conventional control techniques in computer simulations. The controller is based on an idealized model of the manipulator. This is a severe drawback because when the "idealized" con-

Contributed by the Dynamic Systems and Control Division and presented at the Winter Annual Meeting, Boston, Mass., December 14–17, 1987 of The American Society of Mechanical Engineers. Manuscript received at ASME Headquarters May 21, 1987. Paper No. 87-WA/DSC-3.

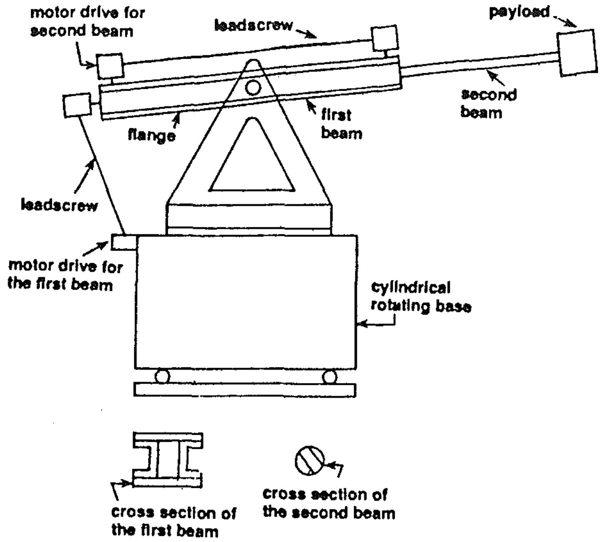

Fig. 1 A schematic of the physical system

trol law is applied on an actual plant, the validity of the scheme will be subject to doubt and the robustness of the controller becomes of great importance.

A time optimal control strategy is studied by Sangveraphunsiri and Book (1982) to enable faster movement of the robot arm. Kahn and Roth (1971) showed that this technique results in a two point boundary value problem. As a consequence, the computation must be repeated for each new set of initial and final conditions used in the numerical solution. In addition, the numerical algorithm yields an optimal solution that is a function of time and does not account for any unexpected disturbances which may act on the system. These drawbacks have rendered the implementation of the time-optimal control technique difficult, if not impossible, for real time application in feedback control of robots. However, this technique has turned out to be a powerful tool for off-line trajectory planning. In an attempt to relax these difficulties, a suboptimal control strategy is often used in digital simulations. In this technique, a linearized version of the dynamic model of the manipulator is obtained for which an analytical optimal control solution can be found.

Many of these sophisticated control techniques suffer from excessive computation time requirements which make them unattractive for real time applications using current microprocessor technology (Wang and Sharma, 1984).

Besides the difficult issues encountered in rigid robots, a new problem is created when robot compliance is included in the dynamic model. It emanates from the distributed nature of the link mass and elasticity. An infinite number of degrees of freedom are required to specify the position of every point on the elastic link. However, due to physical limitations, only a finite number of sensors and actuators can be mounted on the flexible body. Thus resulting in the problem of controlling a large dimensional system with a smaller dimensional controller (Balas, 1978) and (Takahashi et al., 1972).

Two types of forcing functions, to achieve fast response with negligible residual vibrations, are proposed by (Meckl and Seering, 1983) and (Meckl and Seering, 1985). The first type allows vibration to occur during the move but would stop the motion in such a way as to eliminate any residual vibration. The second type avoids the excitation of the resonant modes of the structure as it moves. This work is still at a research level; it can be used off-line to generate the trajectory of the robot arm that satisfies a criterion considering both the time response and the residual vibration.

By and large, the research in the closed loop control of flexible manipulators can be divided into two categories. The first uses additional sensors to measure the flexible motion. That is, all state variables are assumed to be available (Usoro, et al., 1984, Fukuda and Kuribayashi, 1984, Cannon and Schmitz, 1983, Book and Majett, 1982). This enables the inclusion of the flexible motion in the control action, thus achieving better positional accuracy with the existing joint motors. The second category employs a micromanipulator along with additional sensors to compensate for both static and dynamic structural deflections (Zalucky and Hardt, 1982, Cannon et al., 1983, Singh and Schy, 1985). This concept gives the control system designer more capabilities to improve the robot arm performance at additional hardware cost.

Throughout this paper, the term "rigid body controller" is used to refer to the controller whose main objective is to control the rigid body motion of the robot arm, whereas the term "rigid and flexible motion controller" refers to the controller that compensates for both the rigid and flexible motions.

Nomenclature

$(\mathbf{i}, \mathbf{j}, \mathbf{k})$ = noninertial, body fixed, rotating reference frame
m_p = mass of the payload
$q_{1i}(t)$ = flexible motion generalized coordinate in the vertical direction for mode i ($i = 1, 2$)
$q_{2i}(t)$ = flexible motion generalized coordinate in the horizontal direction for mode i ($i = 1, 2$)
r, θ, ϕ = rigid body degrees of freedom of the robot arm
$\mathbf{u}$ = control vector
$\mathbf{x}$ = generalized coordinate vector,
$\mathbf{x}^T$ = $[r, \theta, \phi, q_{11}, q_{12}, q_{21}, q_{22}]$
$(\mathbf{I}, \mathbf{J}, \mathbf{K})$ = inertial reference frame
K^F = feedback gain matrix of the rigid and flexible motion controller
K^R = feedback gain matrix of the rigid body controller
L_1, L_2 = length of the first and second beam, respectively (see Fig. 2)
R_1, R_2, R_3 = desired reference position for r, θ, and ϕ, respectively
$V(y, t)$ = vertical deflection of the end effector
$V(y,t) = \sum_{i=1}^{2} q_{1i}(t)\Phi_i(y)$
$\mathbf{T}$ = joints control torque vector, $\mathbf{T}^T = [T_1, T_2, T_3]$
$\Phi_i(y)$ = spatial function representing the ith elastic mode of a clamped free beam
$(\underset{\sim}{\ })$ = the underbar beneath any variable indicates an n dimensional vector
$(\dot{\ }), (\ddot{\ })$ = a dot or a double dot over any symbol indicates first or second derivative with respect to time in the inertial reference frame

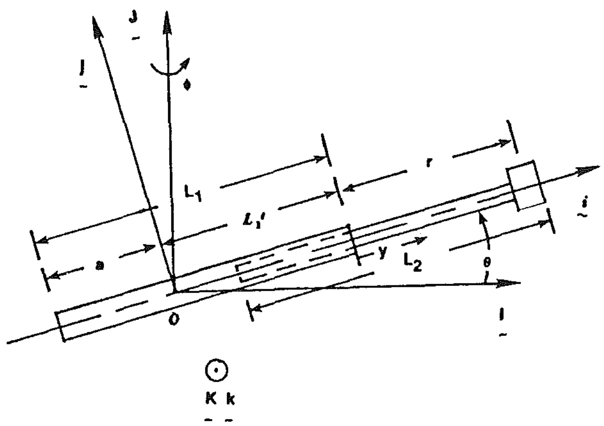

Fig. 2 Arm geometry and coordinates

The purpose of this work is to extend the design of the existing rigid body controllers to include the flexible motion. The rationale is to improve the end effector positional accuracy by damping out the unwanted link vibrations. This is done by using additional sensors to measure the flexible motion and feed it back to the controller. The control action is carried out by the existing joint actuators (i.e., no additional actuators are used).

The spherical coordinate robot arm considered in this study is schematically illustrated in Fig. 1. A derivation of the dynamic model of the robot arm can be found in (Chalhoub and Ulsoy, 1986). A brief description of the physical system along with an outline of the modeling procedure are included in the next section. Subsequently, the design of the "rigid and flexible motion controller" is presented. The simulation results, which illustrate the performance of the controller in the presence of control and observation spillover, are shown in Section 4. In Section 5, the experimental setup is described in some detail. A partial experimental evaluation is performed, in Section 6, to assess the merit of measuring and feeding back the flexible motion. Finally, the work is summarized and the main conclusions are presented.

2 Dynamic Modeling

The physical system considered in this work is a spherical coordinate robot, which has two revolute joints and one prismatic joint (see Fig. 1). All axes are driven by dc servo motors. A gear train is employed to transmit the power from the actuator to the first or the base joint, whereas leadscrew transmission mechanisms are used in the second and third joints. The robot arm is made of two beams such that the second beam can move axially into the first. The length of the first and second beams are denoted L_1 and L_2, respectively, as shown in Fig. 2. A reference inertial frame (**I**, **J**, **K**) fixed at point 0, is shown along with a noninertial, body fixed, rotating reference frame (**i**, **j**, **k**) attached to the first beam. The equations of motion are derived in terms of the latter to keep the mass moment of inertia constant throughout the rigid body motion of the arm.

The robot arm can rotate with angular velocity $\dot{\phi}$ around the vertical axis passing through **J**, and $\dot{\theta}$ around the horizontal axis passing through the pivot point 0 and parallel to the unit vector **k**. The second beam has one additional degree of freedom r which allows it to move axially into the first beam. The payload at the end-of-arm is modeled by a concentrated mass, m_p, at the end of the second beam.

In this study, only the part of the second beam protruding from the first beam is considered to be flexible. The longitudinal vibrations are neglected and only transverse deflections are considered in addition to the rigid body motion. All coupling terms between the rigid and flexible motions are retained. This is done by using a coupled reference position and elastic deformation models. The assumed modes method is employed to represent the deflection of any point on the flexible link. The transverse deflections, in the **j** and **k** directions, are assumed to be dominated by the first two elastic modes. The kinetic and potential energy expressions are then derived. Finally, the Lagrangian approach is used to obtain the unconstrained equations of motion which can be written in the following general form (Chalhoub and Ulsoy, 1986),

$$M(\mathbf{x})\ddot{\mathbf{x}}+F(\mathbf{x},\dot{\mathbf{x}})=F'(\mathbf{T}) \tag{1}$$

where $\mathbf{x}^T = (r, \theta, \phi, q_{11}, q_{12}, q_{21}, q_{22})$ is the generalized coordinate vector. The q_{ij}'s are the time dependent generalized coordinates describing the flexible motion of the last link. $\mathbf{T}^T = [T_1, T_2, T_3]$ is the control torque vector and $M(\mathbf{x})$ is the inertia matrix.

The kinematic constraints associated with the leadscrew transmission mechanisms have also been considered in this work. This is done to investigate the behavior of a leadscrew driven flexible robot arm in the presence of coulomb friction and the self locking condition (i.e., the nonbackdrivability of the leadscrew). The reader is referred to (Chalhoub, 1986) for greater detail on the dynamic model.

3 Controller Design

An integral plus state feedback controller based on a linearized version of the rigid body model of the robot arm has been designed by Chalhoub and Ulsoy (1986). The controller decouples the linearized system, thus allowing a design procedure to be carried out for each axis independently to achieve a damping ratio of $\zeta=1$ and desired servo-loop frequencies of w_{nr}, $w_{n\theta}$, and $w_{n\phi}$ for the r, θ, and ϕ axes, respectively (D'Azzo and Houpis, 1981). This controller is then implemented on the rigid and flexible model. The rationale is to assess the interrelationships between the robot arm structural flexibility and the controller design. The simulation results are discussed in depth in (Chalhoub, 1986).

In this work, the control objective is to introduce additional damping into the flexible motion. This is done by using additional sensors to measure the compliant link vibrations and feed them back to the controller. Note that any compliant link would undergo static and dynamic deflections. There are two approaches with which the static deflection problem can be handled. In the first approach, the static deflection is computed theoretically and then taken into consideration in specifying the desired end effector final position. In the second approach, additional sensors and additional actuators are used. The static deflection is measured and corrected for by the additional actuator referred to as a "straightness servo" in (Zalucky and Hardt, 1982). Here, no attempt is made to compensate for the static deflection, as this can be treated as a separate problem.

Theoretically, any flexible system has an infinite number of elastic modes. Due to physical limitations, a limited number of sensors and actuators can be applied, thus restricting the controller design to a few critical modes. Note that the outputs of the sensors would contain information about the unmodeled as well as the modeled modes. This is referred to as observation spillover. Similarly, the control action would affect both the modeled and unmodeled modes leading to the control spillover. Based on the work done by Balas (1978), the higher unmodeled modes may have a detrimental or destabilizing effect on the system response. To examine the effect of observation and control spillover in the digital simulation, only the first elastic mode in the **j** and **k** directions are considered in the controller design. The second mode is retained in the simulation model and is considered to be representative of the higher unmodeled modes.

The rigid and flexible motion controller is designed based on a linearized version of the equations describing the combined rigid and flexible motions. The linearized equations of motion can be written in the following form,

$$\begin{Bmatrix} \delta\dot{\mathbf{x}} \\ \\ \delta\ddot{\mathbf{x}} \end{Bmatrix} =$$

$$\begin{bmatrix} 0_{5\times5} & I_{5\times5} \\ -M^{-1}(\mathbf{x}_n)\dfrac{\partial F(\mathbf{x}_n,0)}{\partial \mathbf{x}} & -M^{-1}(\mathbf{x}_n)\dfrac{\partial F(\mathbf{x}_n,0)}{\partial \dot{\mathbf{x}}} \end{bmatrix} \begin{Bmatrix} \delta\mathbf{x} \\ \\ \delta\dot{\mathbf{x}} \end{Bmatrix} + \begin{bmatrix} 0_{5\times3} \\ M^{-1}(\mathbf{x}_n)\dfrac{\partial F'}{\partial \mathbf{T}} \end{bmatrix} \delta\mathbf{T} \qquad (2)$$

Define the state vector, $\mathbf{y}$, and the control vector, $\mathbf{u}$, to be:

$$\mathbf{y} = \begin{Bmatrix} \delta\mathbf{x} \\ \delta\dot{\mathbf{x}} \end{Bmatrix}, \text{ and } \mathbf{u} = \delta\mathbf{T} \qquad (3)$$

where $\mathbf{x}^T = (r, \theta, \phi, q_{11}, q_{21})$. The state equations can now be written in the following matrix form,

$$\dot{\mathbf{y}} = A\mathbf{y} + B\mathbf{u} \qquad (4)$$

This represents a linear, time invariant, multi-input multi-output system. Three additional state variables are introduced to facilitate the implementation of the integral plus state feedback controller,

$$y_{11} = \int (r - R_1)dt \quad y_{12} = \int (\theta - R_2)dt$$
$$y_{13} = \int (\phi - R_3)dt \qquad (5a)$$

The augmented state vector becomes

$$\mathbf{y}^T = (r, \theta, \phi, q_{11}, q_{21}, \dot{r}, \dot{\theta}, \dot{\phi}, \dot{q}_{11}, \dot{q}_{21}, y_{11}, y_{12}, y_{13}) \quad (5b)$$

This embeds the integral action into the state equations, thus allowing the control action to be expressed as

$$\mathbf{u} = -K^F\mathbf{y} \qquad (6)$$

where K^F is the feedback gain matrix of the "rigid and flexible motion controller." Substitute (6) into (4), to get

$$\dot{\mathbf{y}} = (A - BK^F)\mathbf{y} \qquad (7)$$

The eigenvalues of the closed loop matrix, $(A - BK^F)$, can be arbitrarily assigned by the controller, defined in (6), as long as the system given by (4) is controllable (Wonham, 1967). Note that for a given set of eigenvalues, the solution for the gain matrix is not unique, since partial assignment of eigenvectors is also required.

The eigenvalues determine the stability and the speed of the response, whereas the closed loop eigenvectors reshape the transient response. The nonuniqueness of the state feedback gain matrix, K^F, in pole assignment provides the designer the freedom to partially select the closed loop eigenvectors (Moore, 1976) and (Chang, 1984).

Standard design procedures (Chen, 1970) employ a transformation matrix to convert the linearized system to controllable canonical form for arbitrary eigenvalue assignment. This converts the multi-input system to single-input one. Then the method established for a single-input system, is implemented to assign the desired closed loop eigenvalues. This methodology does not make any attempt to use the freedom given by the nonuniqueness of the state feedback gain matrix to partially assign the closed loop eigenvectors. Therefore, the shape of the transient response ends up being arbitrarily assigned which leads, in most cases, to poor transient response. This method was employed on the system given by (4). Although, the steady state response followed exactly the reference input, the transient response was very oscillatory. Most of the control effort was assigned to a single component of the control vector, $\mathbf{u}$, thus rendering this particular control design to be completely unacceptable from a practical point of view.

In light of these difficulties, the control problem is now approached from a physical point of view. No transformation matrix is used. Therefore, all the state variables have physical interpretations. The "rigid and flexible motion controller" is obtained by expanding the "rigid body controller", designed by Chalhoub and Ulsoy (1986), with the emphasis on introducing additional damping into the flexible system. An integral plus state feedback controller is used. The integral action is applied on the joint coordinates to insure that they reach their desired values with zero steady state error. To do this, the terms in equation (2), which represent the open loop case have to be physically interpreted. The submatrix $M^{-1}(\mathbf{x})\,\partial F(\mathbf{x},0)/\partial\mathbf{x}$ consists of all the stiffness terms whereas $M^{-1}(\mathbf{x})\,\partial F(\mathbf{x},0)/\partial\dot{\mathbf{x}}$ contains all the damping terms. By evaluating equation (2) and including the integral action, the matrix A in equation (4) becomes

$$A = \left|\begin{array}{ccccc|ccccc|ccc}
0 & 0 & 0 & 0 & 0 & 1 & 0 & 0 & 0 & 0 & 0 & 0 & 0 \\
0 & 0 & 0 & 0 & 0 & 0 & 1 & 0 & 0 & 0 & 0 & 0 & 0 \\
0 & 0 & 0 & 0 & 0 & 0 & 0 & 1 & 0 & 0 & 0 & 0 & 0 \\
0 & 0 & 0 & 0 & 0 & 0 & 0 & 0 & 1 & 0 & 0 & 0 & 0 \\
0 & 0 & 0 & 0 & 0 & 0 & 0 & 0 & 0 & 1 & 0 & 0 & 0 \\
\hline
A_{61} & A_{62} & 0 & A_{64} & 0 & 0 & 0 & 0 & 0 & 0 & 0 & 0 & 0 \\
A_{71} & A_{72} & 0 & A_{74} & 0 & 0 & 0 & 0 & 0 & 0 & 0 & 0 & 0 \\
0 & 0 & 0 & 0 & A_{85} & 0 & 0 & 0 & 0 & 0 & 0 & 0 & 0 \\
A_{91} & A_{92} & 0 & A_{94} & 0 & 0 & 0 & 0 & 0 & 0 & 0 & 0 & 0 \\
0 & 0 & 0 & 0 & A_{10,5} & 0 & 0 & 0 & 0 & 0 & 0 & 0 & 0 \\
\hline
1 & 0 & 0 & 0 & 0 & 0 & 0 & 0 & 0 & 0 & 0 & 0 & 0 \\
0 & 1 & 0 & 0 & 0 & 0 & 0 & 0 & 0 & 0 & 0 & 0 & 0 \\
0 & 0 & 1 & 0 & 0 & 0 & 0 & 0 & 0 & 0 & 0 & 0 & 0
\end{array}\right| \qquad (8)$$

Table 1

Standard Set Of Physical System Parameters	VALUE
Mass of the first beam (m_1)	0.698 Kg
Mass of the second beam (m_2)	0.0429 Kg
Mass of the Payload (m_p)	0.05 Kg
Cross sectional area of the second beam (A_2)	0.00003167 m^2
Length of the first beam (L_1)	0.358 m
Length of the second beam (L_2)	0.5 m
Gravitational acceleration (g)	9.81 m/sec^2
Aluminum density (ρ)	2707 Kg/m^3
Flexural rigidity (EI)	5.67 Pa
Reference position for r	0.4 m
Reference position for θ	0 rad
Reference position for ϕ	0 rad
Desired reference position for r	0.5 m
Desired reference position for θ	0.5 rad
Desired reference position for ϕ	0.5 rad
Servo natural frequency for r(ω_{nr})	4 rad/sec
Servo natural frequency for θ($\omega_{n\theta}$)	4 rad/sec
Servo natural frequency for ϕ($\omega_{n\phi}$)	8 rad/sec
Flexible motion gain, K^F_{19}	-0.000178
Flexible motion gain, K^F_{29}	-0.084
Flexible motion gain, $K^F_{3,10}$	1.568

where the A_{ij}'s represent the open loop terms. Note that $M^{-1}(\mathbf{x})\ \partial F(\mathbf{x},0)/\partial\dot{\mathbf{x}} = 0$; that is no structural damping is considered. This is consistent with the robot arm dynamic modeling assumption. Applying the rigid body controller, derived by Chalhoub and Ulsoy (1986),

$$K^R = \begin{bmatrix} k_{11}^R & k_{12}^R & 0 & 0 & 0 & k_{16}^R & 0 & 0 & 0 & 0 & k_{1,11}^I & 0 & 0 \\ k_{21}^R & k_{22}^R & 0 & 0 & 0 & 0 & k_{27}^R & 0 & 0 & 0 & 0 & k_{2,12}^I & 0 \\ 0 & 0 & k_{33}^R & 0 & 0 & 0 & 0 & k_{38}^R & 0 & 0 & 0 & 0 & k_{3,13}^I \end{bmatrix} \tag{9}$$

where K^R represents the feedback gain matrix of the "rigid body controller." The closed loop matrix $(A - BK^R)$ becomes,

where the α_2 terms represent the additional entries created from the introduction of the "rigid and flexible motion controller" gain matrix. Note that the selection of the gains k_{ij}^F should be done carefully since they simultaneously introduce new terms in the rigid and flexible motion equations. Thus, the larger these gains are, the more damping of the transverse deflections can be achieved, and the greater is the effect of the flexible motion on the rigid body motion. This causes the latter to become oscillatory. Therefore, a compromise should be made in introducing as much damping as possible while keeping the effect of the flexible motion on the rigid body motion to an acceptable small level.

4 Results of the Rigid and Flexible Motion Controller

The "rigid and flexible motion controller" is first applied

$$\left|\begin{array}{ccccc:ccccc:ccc} 0 & 0 & 0 & 0 & 0 & 1 & 0 & 0 & 0 & 0 & 0 & 0 & 0 \\ 0 & 0 & 0 & 0 & 0 & 0 & 1 & 0 & 0 & 0 & 0 & 0 & 0 \\ 0 & 0 & 0 & 0 & 0 & 0 & 0 & 1 & 0 & 0 & 0 & 0 & 0 \\ 0 & 0 & 0 & 0 & 0 & 0 & 0 & 0 & 1 & 0 & 0 & 0 & 0 \\ 0 & 0 & 0 & 0 & 0 & 0 & 0 & 0 & 0 & 1 & 0 & 0 & 0 \\ \hdashline A_{61}-\alpha_1 & A_{62}-\alpha_1 & 0 & A_{64} & 0 & -\alpha_1 & -\alpha_1 & 0 & 0 & 0 & -\alpha_1 & -\alpha_1 & 0 \\ A_{71}-\alpha_1 & A_{72}-\alpha_1 & 0 & A_{74} & 0 & -\alpha_1 & -\alpha_1 & 0 & 0 & 0 & -\alpha_1 & -\alpha_1 & 0 \\ 0 & 0 & -\alpha_1 & 0 & A_{85} & 0 & 0 & -\alpha_1 & 0 & 0 & 0 & 0 & -\alpha_1 \\ A_{91}-\alpha_1 & A_{92}-\alpha_1 & 0 & A_{94} & 0 & -\alpha_1 & -\alpha_1 & 0 & 0 & 0 & -\alpha_1 & -\alpha_1 & 0 \\ 0 & 0 & -\alpha_1 & 0 & A_{10,5} & 0 & 0 & -\alpha_1 & 0 & 0 & 0 & 0 & -\alpha_1 \\ \hdashline 1 & 0 & 0 & 0 & 0 & 0 & 0 & 0 & 0 & 0 & 0 & 0 & 0 \\ 0 & 1 & 0 & 0 & 0 & 0 & 0 & 0 & 0 & 0 & 0 & 0 & 0 \\ 0 & 0 & 1 & 0 & 0 & 0 & 0 & 0 & 0 & 0 & 0 & 0 & 0 \end{array}\right| \tag{10}$$

where the α_1 terms represent the entries altered or created by the introduction of the "rigid body controller". Now, the portion of the closed loop matrix that corresponds to $M^{-1}(\mathbf{x})$ $\partial F(\mathbf{x},0)/\partial\dot{\mathbf{x}}$ has nonzero terms. This represents the damping introduced by the "rigid body controller" in both the rigid and the flexible motions. Since the main objective of the "rigid and flexible motion controller" is to introduce additional damping into the flexible system, then the gain matrix of the "rigid body controller" is modified to give

on a reduced order model where only one elastic mode is considered to represent the flexible motion in each of the **j** and **k** directions. The rationale is to eliminate the effect of observation and control spillover. The standard set of physical system parameters, used in the digitial simulation, are listed in Table 1. Gear's method is employed to solve the highly nonlinear stiff equations describing the combined rigid and flexible motions of the robot arm (Chalhoub, 1986). The responses of the first elastic mode in the **j** and **k** directions are presented in

$$K^F = \begin{bmatrix} k_{11}^R & k_{12}^R & 0 & 0 & 0 & k_{16}^R & 0 & 0 & k_{19}^F & 0 & k_{1,11}^I & 0 & 0 \\ k_{21}^R & k_{22}^R & 0 & 0 & 0 & 0 & k_{27}^R & 0 & k_{29}^F & 0 & 0 & k_{2,12}^I & 0 \\ 0 & 0 & k_{33}^R & 0 & 0 & 0 & 0 & k_{38}^R & 0 & k_{3,10}^F & 0 & 0 & k_{3,13}^I \end{bmatrix} \tag{11}$$

where k_{ij}^R and k_{ij}^I are, respectively, the state feedback and integral action gains of the original "rigid body controller". The k_{ij}^F terms are the new gains introduced to induce additional damping into the flexible motion. The corresponding closed loop matrix, $(A - BK^F)$, can be written as follows

Figs. 3 and 4. The oscillations are due to the inertial forces emanating from the fast and sudden rigid body motions. However, these vibrations rapidly die out; thus reflecting the additional amount of damping introduced by incorporating the flexible motion into the control action.

$$\left|\begin{array}{ccccc:ccccc:ccc} 0 & 0 & 0 & 0 & 0 & 1 & 0 & 0 & 0 & 0 & 0 & 0 & 0 \\ 0 & 0 & 0 & 0 & 0 & 0 & 1 & 0 & 0 & 0 & 0 & 0 & 0 \\ 0 & 0 & 0 & 0 & 0 & 0 & 0 & 1 & 0 & 0 & 0 & 0 & 0 \\ 0 & 0 & 0 & 0 & 0 & 0 & 0 & 0 & 1 & 0 & 0 & 0 & 0 \\ 0 & 0 & 0 & 0 & 0 & 0 & 0 & 0 & 0 & 1 & 0 & 0 & 0 \\ \hdashline A_{61}-\alpha_1 & A_{62}-\alpha_1 & 0 & A_{64} & 0 & -\alpha_1 & -\alpha_1 & 0 & -\alpha_2 & 0 & -\alpha_1 & -\alpha_1 & 0 \\ A_{71}-\alpha_1 & A_{72}-\alpha_1 & 0 & A_{74} & 0 & -\alpha_1 & -\alpha_1 & 0 & -\alpha_2 & 0 & -\alpha_1 & -\alpha_1 & 0 \\ 0 & 0 & -\alpha_1 & 0 & A_{85} & 0 & 0 & -\alpha_1 & 0 & -\alpha_2 & 0 & 0 & -\alpha_1 \\ A_{91}-\alpha_1 & A_{92}-\alpha_1 & 0 & A_{94} & 0 & -\alpha_1 & -\alpha_1 & 0 & -\alpha_2 & 0 & -\alpha_1 & -\alpha_1 & 0 \\ 0 & 0 & -\alpha_1 & 0 & A_{10,5} & 0 & 0 & -\alpha_1 & 0 & -\alpha_2 & 0 & 0 & -\alpha_1 \\ \hdashline 1 & 0 & 0 & 0 & 0 & 0 & 0 & 0 & 0 & 0 & 0 & 0 & 0 \\ 0 & 1 & 0 & 0 & 0 & 0 & 0 & 0 & 0 & 0 & 0 & 0 & 0 \\ 0 & 0 & 1 & 0 & 0 & 0 & 0 & 0 & 0 & 0 & 0 & 0 & 0 \end{array}\right| \tag{12}$$

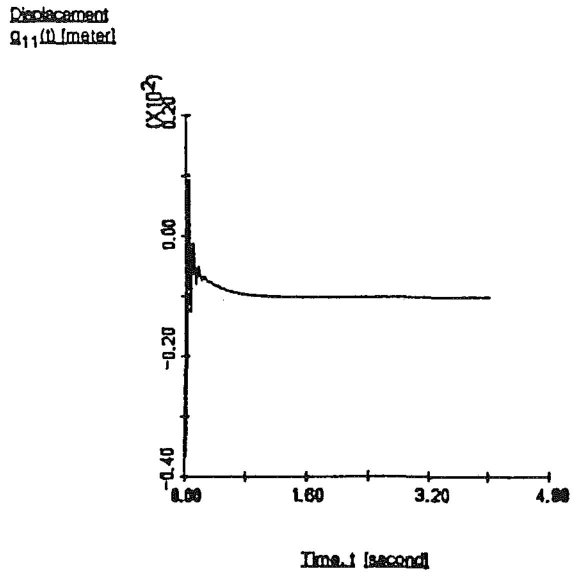

Fig. 3 Flexible motion coordinate, $q_{11}(t)$, in response to the rigid and flexible motion controller in the reduced order model case

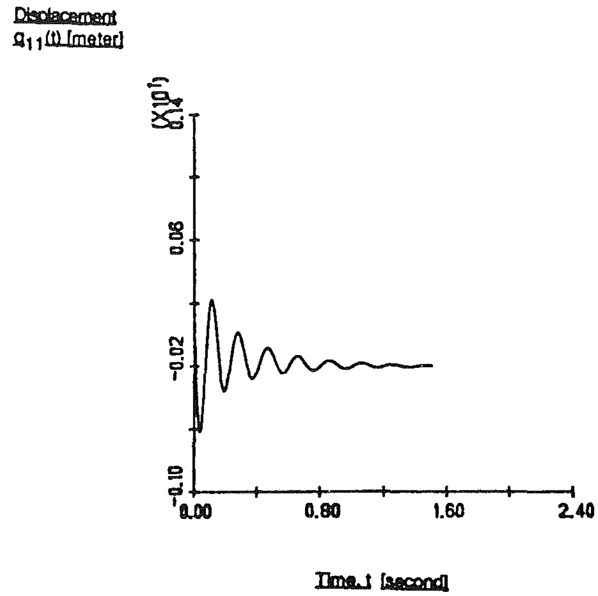

Fig. 5 Flexible motion coordinate, $q_{11}(t)$, in response to the rigid and flexible motion controller in the control spillover case

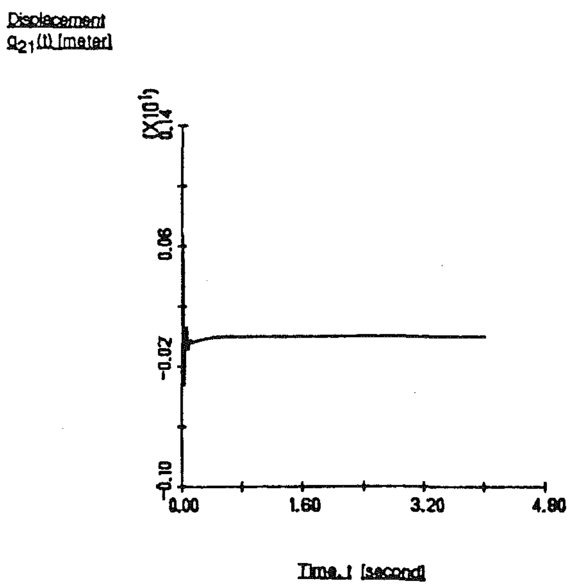

Fig. 4 Flexible motion coordinate, $q_{21}(t)$, in response to the rigid and flexible motion controller in the reduced order model case

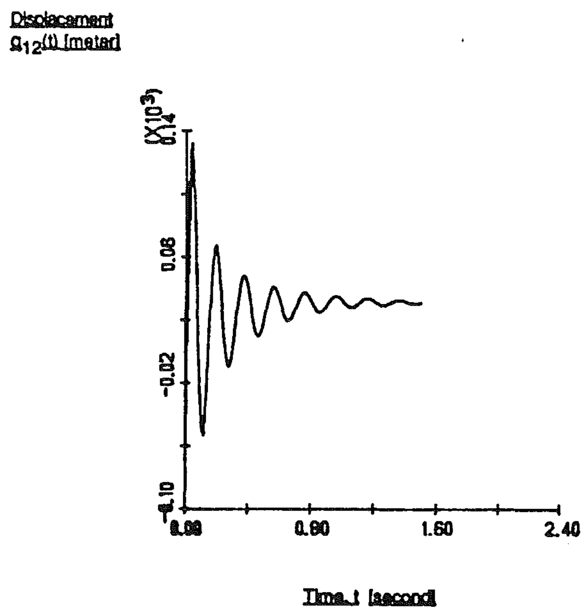

Fig. 6 Flexible motion coordinate, $q_{12}(t)$, in response to the rigid and flexible motion controller in the control spillover case

Additional simulation runs are made to study the following effects:

(1) Control spillover: The "rigid and flexible motion controller" is now applied to the full dynamic model of the robot arm which employs two elastic modes to represent the transverse vibration in each of the **j** and **k** directions. This is done to assess the effect of control spillover on the second uncontrolled elastic mode. Representative results are shown in Figs. 5 and 6. They represent the response of the first and second elastic mode of the flexible motion in the **j** direction. Due to the control spillover, the response corresponding to the first mode becomes more oscillatory than in the previous case. However, the overall performance of the flexible motion coordinates shows a reduction of approximately 50 percent in magnitude when compared with their counterparts in the base run (Chalhoub and Ulsoy, 1986), which illustrates the behavior of the robot arm in response to the "rigid body controller."

(2) Control and observation spillover: This run simulates an actual situation where both control and observation spillover can be present. The generalized coordinates $q_{11}(t)$ and $q_{21}(t)$, that are fed back to the controller and which represent the first elastic mode of the flexible motion in each of the **j** and **k** directions, are no longer representative of the first mode only. Instead, they contain information about both the first and second elastic modes. The responses of the first mode in the **j** and **k** directions are almost identical to those in the control spillover case. The uncontrolled second elastic mode of the flexible motion in the **j** direction becomes unstable (see Fig. 7). This is as predicted by Balas (1978). The instability is obtained due to the combined effect of control and observation spillover on the second mode.

(3) Control and observation spillover in the presence of structural damping: Fortunately, any physical system

inherently possesses a certain amount of structural damping. As suggested by Balas (1978), the structural damping provides a margin of stability for the uncontrolled modes. This is investigated by using Rayleigh's dissipation function to introduce very light structural damping, $\zeta = 0.0145$, into the dynamic model of the flexible robot arm. The results are identical to their counterparts in the undamped model with control and observation spillover except for the response of the second elastic mode in the **j** direction, $q_{12}(t)$. The plot, shown in Fig. 8, illustrates the strong interaction between the structural damping of the robotic manipulator and the detrimental effect of observation and control spillover on the uncontrolled elastic modes.

A numerical comparison, based on the measurement of the settling time for the end effector deflection in the **j** direction, is made between the results obtained by Chalhoub and Ulsoy (1986) for the "rigid body controller" and those of the "rigid and flexible motion controller". The tolerance used in determining the settling time is ±0.1mm from the static deflection position of the end effector; which corresponds to −4.1mm. The numerical values show a significant reduction in the settling time from 3.5 s in the "rigid body controller" case to 1.0657 s in the "rigid and flexible motion controller" case.

5 Experimental Setup

The three degree of freedom spherical coordinate laboratory robot, described in Section 2, is used for the experimental work. It is interfaced to an IBM/XT personal com-

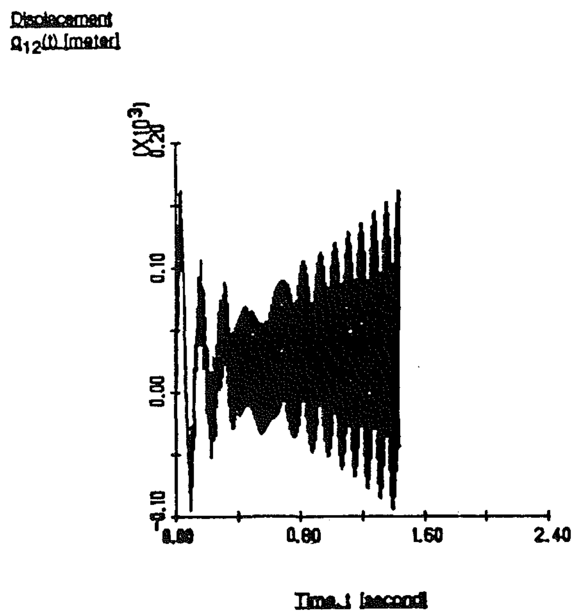

Fig. 7 Flexible motion coordinate, $q_{12}(t)$, in response to the rigid and flexible motion controller in the control and observation spillover case

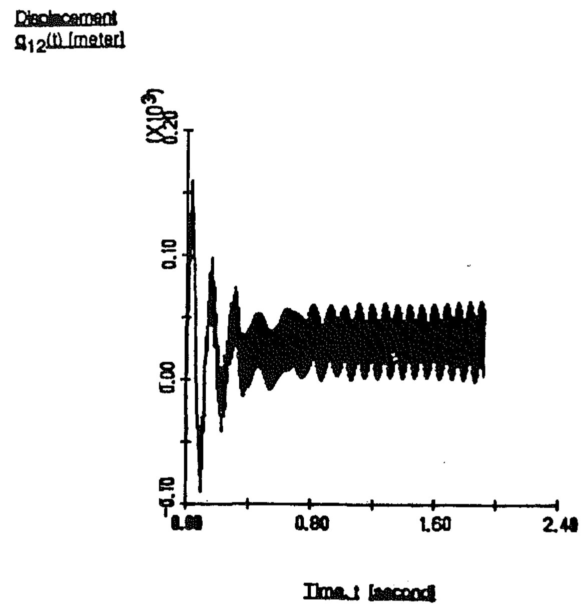

Fig. 8 Flexible motion coordinate, $q_{12}(t)$, in response to the rigid and flexible motion controller in the control and observation spillover with structural damping included

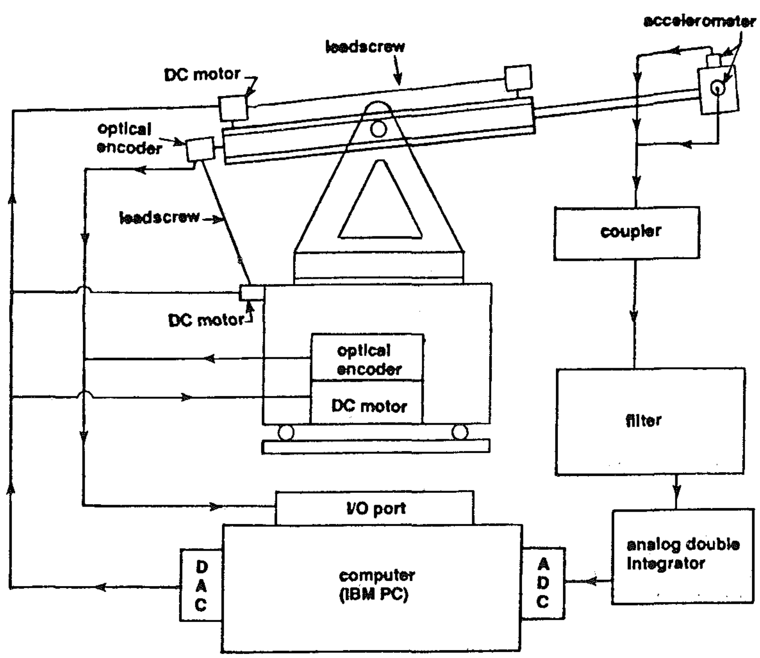

Fig. 9 A schematic of the experimental setup

puter whose capabilities are enhanced by a Tecmar Lab Tender interface board. The latter has built-in 8 bit analog to digital and digital to analog converters. The schematic of the experimental setup is given in Fig. 9. Three dc servo motors, driven by power amplifiers, are used as actuators. The control torques are transmitted to the joints by leadscrews for the r and θ axes and a gear train for the ϕ axis. One tachometer generator and one optical encoder (Rangan, 1982, and Desilva, 1985) are mounted on each joint to measure the position and velocity of its corresponding rigid body degree of freedom. The optical encoder signals are read by the computer through digital counters. Each joint has a different number of counters associated with it according to their range of operation. A twenty bit counter is used to record the number of counts generated by the optical encoder monitoring the ϕ rotation whereas 12 bit and 20 bit counters are used to record the θ and r motions, respectively. The contents of each counter are strobed into a tristate buffer which can be accessed by the computer through differential drivers. Differential receivers are also used to reduce the noise on the control lines originating with the microcomputer.

The part of the second beam protruding from the first beam, which is considered to be flexible in the digital simulation, is constructed of a thin aluminum rod. The payload is kept constant. Its total mass is 0.08 Kg, and it consists of a mounting stud and two orthogonally mounted Kistler piezotron accelerometers (model 8606A100). They are used to measure the end effector transverse vibrations in both the **j** and **k** directions. The stability conditions for such systems where the sensors are not colocated with the actuators are discussed in (Gervater, 1970). The acceleration signals are passed through a Kistler piezotron coupler (model 5120) which has a built-in Kistler low pass filter (model 5318A22) with a break frequency set to 60 Hz. This attenuates the higher mode signals, thus reducing the effects of observation spillover. The dc component of the couplers output needs to be filtered out. It represents the end effector acceleration due to the rigid body motion. This is done by passing the acceleration signals through two cascaded high pass Krohn-Hite filters (model 3322) with a break frequency set to 3 Hz. Finally, the total deflection of the end effector and its time rate are obtained by integrating twice the accelerometer signals using analog double integrators (Holman, 1978) and (Hayt and Kemmerly, 1978). This is done in order to devote most of the sampling period to the computation of the control action. The flexible motion signals are then digitized by the 8 bit analog to digital converter.

The speed of the microcomputer imposes a stringent constraint on the design of the second beam. In the experimental work, the flexible motion is considered to be dominant by the first elastic mode. To avoid aliasing (Franklin and Powell, 1981), the sampling theorem must be satisfied. That is, the sampling period must be, at most, half the fundamental period. Thus, the fundamental frequency, which is fixed once a certain design for the second beam is adopted, would set the maximum sampling period. However, for a high fundamental frequency, the period, which is inversely proportional to the natural frequency, becomes very small. Depending on the speed of the microcomputer or the control algorithm used, the upper bound of the sampling period imposed by the design of the second beam, may or may not be large enough to perform the necessary control calculations at each step. Therefore, in this work, the second beam is designed to have a low fundamental frequency. For the experimental setup employed here, the length of the second beam is chosen to be 0.5 m and its diameter is 0.635 cm so that its fundamental frequency is approximately 6 Hz. The sampling period used is 0.024 s which is well below the upper bound imposed by the sampling theorem.

Due to the computational speed limitations of the microcomputer used, a complete validation of the three degrees of freedom spherical coordinate robot arm with a flexible link could not be undertaken. A partial experimental validation was performed by controlling the θ joint and the flexible motion in the **j** direction only. r and ϕ were held fixed during the experiments. Although a complete experimental validation is desirable, this limited experimental study addresses the main focus of the paper. That is, the use of joint actuators to simultaneously control the joint motion and reduce structural vibrations by feeding back both joint and end-of-arm motions. The θ motion is measured using an optical encoder with 625 counts per revolution (Optisyn model 77-4-003-625AA). Its resolution is enhanced by connecting the encoder shaft to a gear train with a gear ratio of 18:1. This yields a resolution of 31.25 counts per degree of θ.

6 Results of the Experimental Work

In contrast to the digital simulation, the limited scope of the experimental study (i.e., r and ϕ fixed) can only provide partial evaluation of the performance of the proposed approach. The dynamics of the actuators and sensors are considered in the controller design for the experimental system. The robot arm is treated as a pure inertia loading on the motor shaft. The armature controlled dc motor used in the experimental setup is very common in servo controlled systems. The derivation of its dynamic model is well documented in the literature (D'Azzo and Houpis, 1981). The corresponding transfer function for the θ axis can be written as follows

$$\frac{\omega(s)}{u(s)}=\frac{K}{\tau s+1} \tag{13}$$

where s is the Laplace transform variable, $\omega(s)$ is the Laplace transformed axis velocity $\dot{\theta}(t)$, and $u(s)$ is the input voltage to the motor, τ is the time constant and K is the overall gain of the motor, the power amplifier, and the tachometer generator. Several open loop runs are made, where different step inputs are given to the system and the sensors values are stored in the computer. The average values for the overall gain, K, and the system time constant, τ, are found to be 2.284 degree/s/volt and 0.15 s, respectively.

First the "rigid body controller" is applied on the robot arm to rotate it from its initial position $\theta(0)=0$, which corresponds to the horizontal position, to a certain desired position, R_2. The numerical values used in the "rigid body controller' gain matrix are,

$$K^R=[-57.37\ -8.75\ -51.52] \tag{14}$$

It is found that for R_2 greater than 20 degrees the effect of nonlinearities become significant and the response is oscillatory. Typical results of the "rigid body controller" for $R_2=-20$ degrees are shown in Figs. 10 and 11. The first plot shows the θ response. It has a small overshoot which persists for a while due to the effect of coulomb friction. Figure 11 represents the dynamic deflection of the end effector in the **j** direction. The control signal, which is not included here due to space limitations, shows some saturation. This is desirable since it serves the purpose of driving the robot arm at its highest speed. It is also evident from Fig. 11 that there is significant quantization error due to the poor resolution obtained from the 8 bit analog to digital and digital to analog converters.

Next the "rigid and flexible motion controller" is applied. The objective is to introduce additional damping into the flexible motion. This is done by following the same control design approach used in Section 3. That is expanding the "rigid body controller" to include the feedback signal of the first elastic

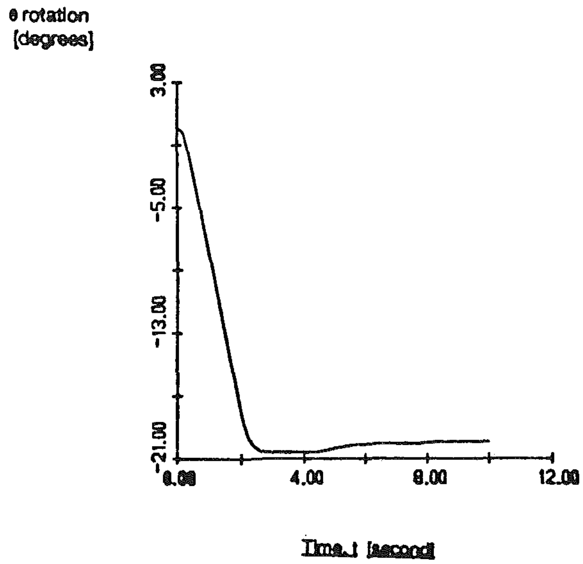

Fig. 10 θ response obtained from the rigid body controller in the experimental work

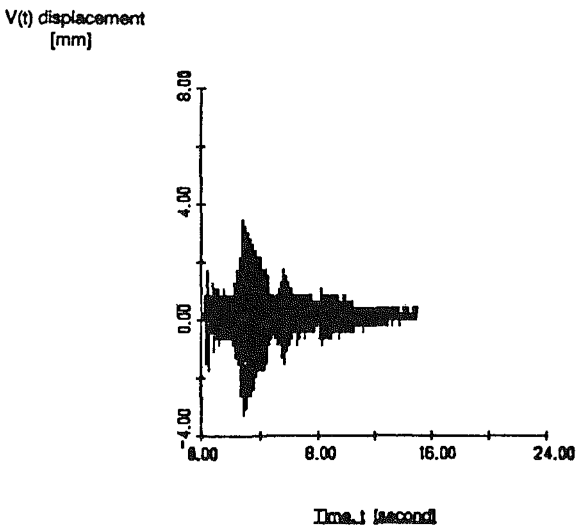

Fig. 11 Total vertical deflection in response to the rigid body controller in the experimental work

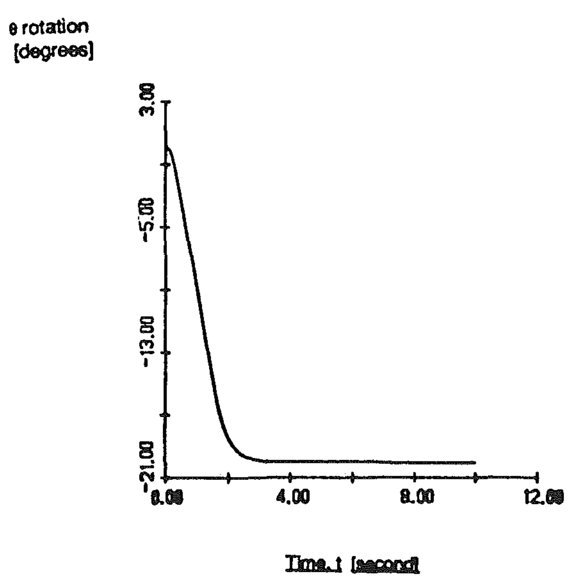

Fig. 12 θ response obtained from the rigid and flexible motion controller in the experimental work

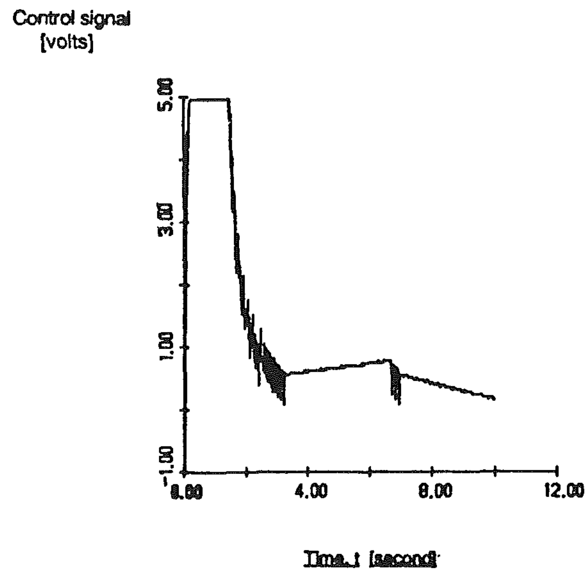

Fig. 13 Control signal for the second joint obtained from the rigid and flexible motion controller in the experimental work

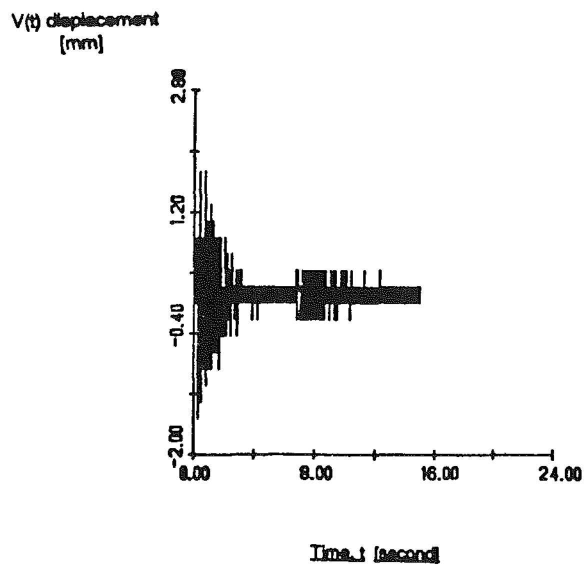

Fig. 14 Total vertical deflection in response to the rigid and flexible motion controller in the experimental work

mode of the flexible motion in the **j** direction. The gain matrix of the "rigid and flexible motion controller" is,

$$K^F = [-57.37\ -8.75\ -51.52\ -30.00] \qquad (15)$$

In the experimental work, the observation and control spillover are always present. The control action affects all elastic modes and the accelerometer output contains some information about all modes. A low pass filter with a break frequency set to 60 Hz attenuates the effect of higher modes. However, it does not eliminate the observation spillover problem entirely. Fortunately, the physical system exhibits light structural damping. As seen from the digital simulation results, this can provide a margin of stability for the uncontrolled modes due to the strong interaction between the structural damping and the detrimental effect of observation and control spillover.

The results of the "rigid and flexible motion controller" are shown in Figs. 12 to 14. The first plot represents the overdamped θ response. The control signal, shown in Fig. 13, fluctuates sharply during the period where θ approaches its desired value. In response to these oscillations, the dc motor in-

Table 2

	settling time (seconds)	maximum deflection (peak to peak)
rigid body controller	11.0	7.5mm
rigid and flexible motion controller	3.0	2.7mm

troduces a series of pulses into the system. This produces additional damping into the flexible motion which results in a reduction of the amplitude of the dynamic deflection in the **j** direction. This is illustrated in Fig. 14 where the maximum amplitude of the end effector is reduced by approximately 75 percent as compared to the "rigid body controller" result shown in Fig. 11. It is clear that the joint actuators must have adequate bandwidth to generate the high frequency input required to damp the flexible motion.

Numerical values for the settling time (for a ± 0.3 mm band) and the maximum deflection of the end effector in the **j** direction are given in Table 2 for both the "rigid body controller" and the "rigid and flexible motion controller". The comparison of the numerical values shows a significant reduction in both the maximum deflection and the settling time.

7 Summary and Conclusions

The dynamic model presented in Chalhoub and Ulsoy (1986), for a spherical coordinate robot arm whose last link only is considered to be flexible, is used in this work to evaluate the performance of a "rigid and flexible motion controller". The latter is obtained by extending the integral plus state feedback controller, derived for the rigid body model of the robot arm (Chalhoub and Ulsoy, 1986), to include the flexible motion. The rationale is to introduce additional damping into the flexible motion. This is done by using additional sensors to measure the compliant link vibrations and feed them back to the controller. Only the existing joint actuators are employed. The effect of the control and observation spillover is examined by considering one elastic mode in the **j** and **k** directions in the controller design. A second mode is included in the dynamic model, and is considered to be representative of the higher unmodeled modes. Finally, partial experimental evaluation is performed on both the "rigid and flexible motion controller" and the "rigid body controller" to assess the merit of measuring and feeding back the flexible motion.

The simulation results show that additional damping in the flexible motion can be achieved by including the flexible motion in the control action. The strong interaction between the structural damping of the manipulator and the detrimental effect of observation and control spillover is also demonstrated.

An experimental study is conducted to partially evaluate the performance of this approach. Both controllers, the "rigid body controller" and the "rigid and flexible motion controller", are tested on a single joint of a spherical coordinate laboratory robot arm. The experimental results show a significant reduction in the end effector dynamic deflection. The important issue of observation and control spillover is examined. It is found to present no significant practical problem in the presence of light structural damping, provided adequate filtering of the vibration measurement signal and proper choice of sensor and actuator locations are made. This partially validates the digital simulation results.

In conclusion, the introduction of the flexible motion into the control action, by using the existing joint actuators and both joint and end-of-arm motion sensors, has improved the positional accuracy of the end effector by reducing the settling time for the unwanted residual vibrations. However, the joint actuators must have adequate bandwidth to generate the high frequency input required to damp out the flexible motion.

Acknowledgment

The authors are pleased to acknowledge the financial support of the Center for Research and Integrated Manufacturing at the University of Michigan, and the United States Air Force Office of Scientific Research under contract number F49620-82-C-0089. They also thank John Caldwell, Jerry Turney and Rob Giles for their technical assistance in the experimental work, Mary English for assistance with the preparation of this manuscript, and the reviewers for their helpful comments.

References

Balas, M., 1978, "Feedback Control of Flexible Systems," *IEEE Transactions on Automatic Control*, Vol. AC-23, No. 4, Aug.

Balestrino, A., De Maria, G., and Sciavicco, L., 1983, "An Adaptive Model Following Control for Robotic Manipulators," ASME Journal of Dynamic Systems, Measurement, and Control, Vol. 105, Sept., pp. 143-151.

Book, W. J., and Majett, M., 1982, "Controller Design for Flexible, Distributed Parameter Mechanical Arms Via Combined State Space and Frequency Domain Techniques," in *Robotics Research and Advanced Applications*, Book, W. J. (ed.), ASME Booklet, Nov., pp. 101-120.

Cannon, R. H., and Schmitz, E., 1983, "Initial Experiments on the End-point Control of a Flexible One Link Robot," *The International Journal of Robotics Research*, Nov.

Cannon, R. H., et al., 1983, First Annual Report of the Center for Automation and Manufacturing Science, Stanford University, Nov.

Chalhoub, N. G., 1986, "Control of a Leadscrew Driven Flexible Robot Arm," Ph.D. thesis, University of Michigan, May.

Chalhoub, N. G., and Ulsoy, A. G., 1986, "Dynamic Simulation of a Flexible Robot Arm and Controller," ASME Journal of Dynamic Systems, Measurement, and Control, June.

Chang, M. J., 1984, "Eigenstructure Assignment by State Feedback," *Proceedings of the 1984 American Control Conference*, Vol. 1, pp. 372-377.

Chen, C. T., 1970, *Introduction to Linear Systems Theory*, Holt, Rinehart and Winston.

D'Azzo, J., and Houpis, C. H., 1981, *Linear Control System Analysis and Design*, McGraw-Hill, New York.

Desilva, C. W., 1985, "Motion Sensors in Industrial Robots," *Mechanical Engineering*, June, pp. 40-51.

Donalson, D. D., and Leondes, C. T., 1963, "A Model Referenced Parameter Tracking Technique for Adaptive Control Systems: Part I – The Principles of Adaptation and Part II – Stability Analysis by the Second Method of Lyapunov," *IEEE Transactions on Applications and Industry*, Vol. 82, No. 68, Sept., pp. 241-262.

Dubowsky, S., and Desforges, D. T., 1979, "The Application of Model-Reference Adaptive Control to Robotic Manipulators," ASME Journal of Dynamic Systems, Measurement, and Control, Vol. 101, No. 3, Sept., pp. 193-200.

Franklin, G. F., and Powell, J. D., 1981, *Digital Control of Dynamic Systems*, Addison-Wesley, June.

Fukuda, T., and Kuribayashi, Y., 1984, "Flexibility Control of Elastic Robotic Arms and Its Application to Contouring Control," *IEEE Computer Society, International Conference on Robotics*, Atlanta, Mar.

Gervater, W. B., 1970, "Basic Relations for Control of Flexible Vehicles," *AIAA Journal*, Vol. 8, No. 4, Apr., pp. 666-672.

Gilbert, E., and Ha, I. J., 1984, "An Approach to Nonlinear Feedback Control With Applications to Robotics," *IEEE Transactions on Systems, Man, and Cybernetics*, Vol. SMC-14, No. 6, Nov/Dec., pp. 879-884.

Hayt, W. H., and Kemmerly, J. E., 1978, *Engineering Circuit Analysis*, McGraw-Hill, Third Edition.

Holman, J. P., 1978, *Experimental Methods for Engineers*, McGraw-Hill, Third Edition.

Horowitz, R., and Tomizuka, M., 1980, "An Adaptive Control Scheme for Mechanical Manipulators – Compensation of Nonlinearity and Decoupling Control," ASME Paper No. 80-WA/DSC-6.

Kahn, M. E., and Roth, B., 1971, "The Near-Minimum Time Control of Open-Loop Articulated Kinematic Chains," ASME Journal of Dynamic Systems, Measurement, and Control, Sept.

Landau, Y. D., 1979, *Adaptive Control Systems*, Marcel Dekker.

Lee, C. S. G., and Lee, B. H., 1984, "Resolved Motion Adaptive Control for Mechanical Manipulators," ASME JOURNAL OF DYNAMIC SYSTEMS, MEASUREMENT, AND CONTROL, Vol. 106, June., pp. 134–142.

Meckl, P. H., and Seering, W. P., 1983, "Active Damping in a Three-Axis Robotic Manipulator," Presented at the Ninth ASME Vibration Conference, Dearborn, MI, Sept.

Meckl, P. H., and Seering, W. P., 1985, "Minimizing Residual Vibration for Point to Point Motion," ASME Paper No. 85-DET-17.

Moore, B. C., 1976, "On the Flexibility Offered by State Feedback in Multivariable Systems Beyond Closed Loop Eigenvalue Assignment," *IEEE Transactions on Automatic Control*, Vol. AC-21, Oct., pp. 689–692.

Rangan, K. V., 1982, "Position and Velocity Measurement by Optical Shaft Encoders," Robotics Institute, Carnegie-Mellon University, Pittsburgh, Pennsylvania, June.

Sangveraphunsiri, V., and Book, W. J., 1982, "An Approach to the Minimum Time Control of a Simple Flexible Arm," in *Robotics Research and Advanced Applications*, Book, W. J. (ed.), ASME Booklet, Nov., pp. 219–232.

Singh, S. N., and Schy, A. A., 1985, "Decomposition and State Variable Feedback Control of Elastic Robotic Systems," *Proceedings of the 1985 American Control Conference*, Vol. 2, Boston, MA, pp. 375–380.

Takahashi, Y., Rabins, M., and Auslander, D., 1972, *Control and Dynamic Systems*, Addison-Wesley, Nov., pp. 431–452.

Usoro, P. B., Nadira, R., and Mahil, S. S., 1984, "Control of Lightweight Flexible Manipulators: A Feasibility Study," *Proceedings of the 1984 American Control Conference*, Vol. 2, San Diego, Calif., pp. 1209–1216.

Wang, S. S., and Sharma, A., 1984, "Dynamic Control Models of a Robot for High Speed and High Precision Assembly With Tolerance Constraints," *Proceedings of the 1984 American Control Conference*, Vol. 2, San Diego, Calif., pp. 872–877.

Wonham, W. M., 1967, "On Pole Assignment in Multi-Input Controllable Linear Systems," *IEEE Transactions on Automatic Control*, Vol. AC-12, No. 6, Dec., pp. 660–665.

Zalucky, A., and Hardt, D. E., 1982, "Active Control of Robot Structure Deflections," in *Robotics Research and Advanced Applications*, Book, W. J. (ed.), ASME Booklet, Nov., pp. 83–100.